

Tuning of Nonvolatile Bipolar Memristive Switching in Co(III) Polymer with an Extended Azo Aromatic Ligand

Anasuya Bandyopadhyay,[†] Satyajit Sahu,[‡] and Masayoshi Higuchi^{*,†}

[†]International Center for Material Nanoarchitectonics (MANA), National Institute for Material Science (NIMS), 1-1 Namiki, Tsukuba 305-0044, Japan

[‡]Advanced Nano Characterization Center, NIMS, 1-2-1 Sengen, Tsukuba, 305-0047, Japan

 Supporting Information

ABSTRACT: We have fabricated a unique memristive device by molecular engineering and demonstrated that the leakage current tuning in the device is 100 times more efficient than that in a standard device. Molecular analogs of the memristive matrices used here are an electrochemically active conjugated Co(III) polymer (CP) and a nonconjugated Co(III) polymer (NCP), which have been synthesized in good yield and characterized by ¹H NMR spectroscopy. Redox switching of an organic–metallic hybrid polymer generates bistable states with a large ON/OFF ratio that supports random flip-flops for several hours. Thus, we provide a synthetic solution to leakage current restriction, one of the fundamental problems faced when fabricating state-of-the-art electronic devices.

The exponential increase in information communication¹ has resulted in an urgent demand for a new technique for fabricating memory-switching devices.² In 1971, Leon O. Chua proposed a new circuit element,³ a memristor, which is the latest addition to the existing list of electronic devices (resistor, capacitor, and inductors). A memristor is capable of processing information as are biological systems. Recently, this conceptual device has been explored in a doped titanium dioxide matrix.⁴ It has also been shown that the hysteresis in current–voltage (*I*–*V*) characteristics can be used to emulate neural networks.⁴ To make further improvements to the memristor architecture, it is necessary to explore various avenues of atomic engineering.

In general, a majority of the polymer materials with electrical switching characteristics lack proper atomic engineering in its fundamental information processing part. Recently studied polymer systems have intriguing memory switching characteristics that result from charge transfer,⁵ metal-filament growth,⁶ conformational change,⁷ ion motion,⁸ dynamic doping,⁹ and charge trapping.¹⁰ Further, molecular switching has been reported by tuning the reversible redox activity of a functional moiety.¹¹ In addition, a combination of conjugated and nonconjugated molecular structures has been used for designing a molecular rectifier¹² to the logic gate.¹³ In this study, we have combined these two concepts to design a molecular analog of the recently invented memristor device.³ To be specific, we replicate the potential distribution in a typical dopant-titania complex used to fabricate a memristive device, by employing an aromatic ligand in

which two conjugated aromatic moieties are separated by a nonconjugated aliphatic moiety. In a typical memristive device, the metal ion dopants are randomly distributed in the matrix.^{3,14} We attempted to mimic such a distribution by synthesizing a metal–organic hybrid polymer, in which a metal ion is directly bonded to an organic ligand. Therefore, the atomic-scale potential distribution is more organized in this polymer as compared to that in a dopant-titania film³ or a conventional memristor matrix.¹⁴

It is known that metal coordination complexes¹⁵ and azo-benzene-containing polymers¹⁶ show memory-switching behavior. In this study, we modify the functional groups in an ionic coordination complex, so that the properties of the memristor based on this complex can be appropriately tuned. We report the design/synthesis and electronic memory of a cobalt(III)-containing conjugated (CP) and nonconjugated polymer (NCP) with an azo-aromatic backbone.

Co monomer (**1**) was synthesized by following a previously reported procedure¹⁷ using 1,4-phenylene diamine as the primary amine. In the subsequent step, the desired polymer (**2**) was prepared by refluxing **1** with terephthalaldehyde in dehydrated ethanol for 48 h in the presence of a dehydrating agent such as Si(OEt)₄ (Figure 1). The desired polymer was isolated as a bright-green solid in 77% yield, and it was found to be soluble in all common organic solvents except methanol. The oxidation state of Co in the monomer and both polymers was +3. The azo ligand was monoanionic, and one perchlorate ion remained outside the coordination sphere. The structure of the polymer was confirmed by ¹H NMR analysis. The peaks at δ10.003 and δ5.73 corresponded to the single proton of the terminal terephthalaldehyde moiety and that of the terminal Co-moiety, respectively. The aldehyde proton in the polymer was shifted upfield because of the replacement of the more electronegative oxygen atom by a less electronegative nitrogen atom (see Figures S1 and S2 in the Supporting Information, SI). The characterization of these two terminal peaks confirmed the formation of a 1:1 Co monomer/terephthalaldehyde complex. Identification of the above-mentioned terminal groups helped in the integration of the other polymer peaks with respect to the terminal-group peaks; further, the formation of an 18-mer was confirmed from integration. From these data, we could conclude that the resulting conjugated polymer had an average molecular weight of 15 kg/mol. The NCP was also synthesized by following the same procedure using glutaraldehyde as the spacer group. When the

Received: August 3, 2010

Published: January 6, 2011

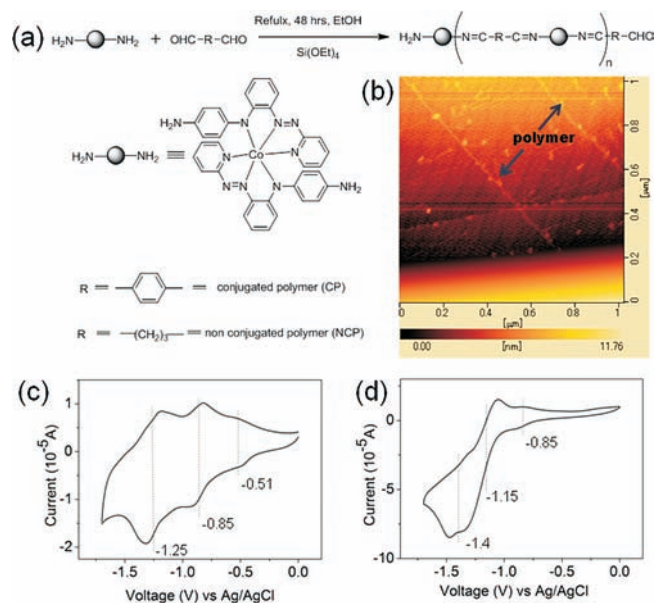


Figure 1. (a) Synthesis of Co(III) polymer of azo aromatic ligand. (b). AFM image for CP (c) cyclic voltammogram of Co monomer and (d) cyclic voltammogram (CV) of CP.

aromatic spacer group was replaced with an aliphatic group, a marked change in the solubility of the polymer was observed; the resulting polymer was soluble only in high-boiling solvents such as DMSO and DMF and insoluble in all common organic solvents. The NMR peak pattern for the NCP was very similar to that in the aromatic region of the CP, and the average molecular weight of the NCP was estimated by NMR to be 10.6 kg/mol (SI Figure S3).

The monomer and the polymers (CP and NCP) showed reversible cyclic voltammograms (CV); a Ag/AgCl electrode was used as the reference electrode (Figure 1c, d and SI Figure S4 for (NCP)). The first cathodic response in the case of the monomer was due to the reduction of Co(III) to Co(II), while the second and third cathodic responses were attributed to the stepwise reduction of the two coordinated azo ligands. In addition to these three cathodic responses, both of the polymers showed two more peaks attributable to the reduction of the two newly formed C=N bonds. The first C=N reduction peak overlapped with the second azo-reduction peak. The voltammogram of the NCP was similar, but the peak positions were different.

To gain a better understanding of the electrochemical properties of Co complexes, we isolated the azo ligand (SI Figure S5a) from the Co monomer¹⁸ and studied its electrochemical properties. The voltammogram of the ligand shows only one reversible cathodic peak at -1.1 V (SI Figure 5b); this peak is due to the reduction of the azo group. In all Co complexes (**1**, **2**, **3**), the potential of this particular peak is shifted toward at more positive value (-0.85 V) because of the strong electronic pull of the higher-valent metal ion (Co^{3+}). After coordination with Co^{3+} , the azo ligand becomes electron deficient and hence is more easily reduced than the free (uncoordinated) ligand. Therefore, from the CV of the free ligand, it is apparent that the first electronic response in the case of all metal complexes is due to the reduction of Co(III) to Co(II).

The memristor device was fabricated in the following manner. Acetonitrile and DMSO solutions of the CP and NCP, respectively, were dropped onto a Si/SiO₂ substrate and dried.

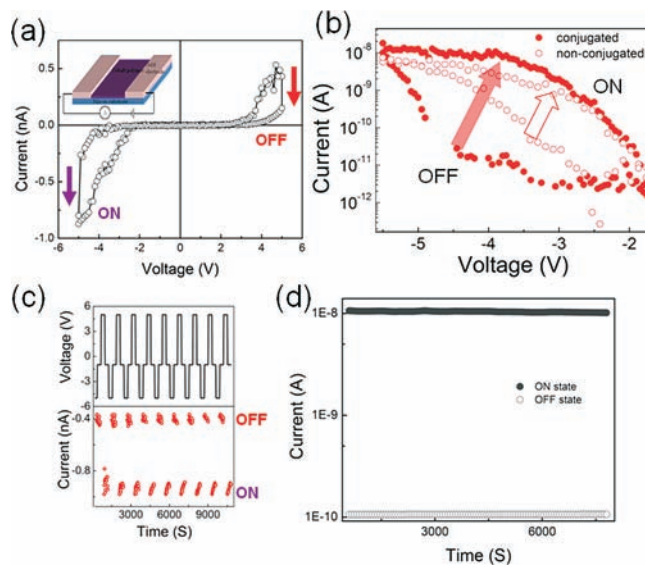


Figure 2. (a) I - V characteristic of CP device, arrow denotes switching direction. Inset shows lateral device scheme. (b) Comparative logarithmic current of CP and NCP devices ($V_{\text{max}} \sim 5.5$ V). (c) Current responses during the write-read-erase-read voltage cycle. (d) Retention time of the on- and off-state data of CP device.

Interdigitated Au electrodes (lateral gap ~ 200 nm) were fabricated on the substrate by e-beam lithography. To suppress the formation of pinning-effect-induced artifacts during comparison,¹⁹ a lateral structure was adopted instead of a sandwich structure, although the latter showed superior performance (SI Figure S6). All the I - V characteristics were measured in an ambient atmosphere by using an Agilent 4155c semiconductor parameter analyzer attached to a Vector probe station.

The I - V curve was traced in the range $V_{\text{max}} = 5$ V to -5 V at a scan rate of 20 mV/s, with a potential sweep from a positive to negative direction. Figure 2a shows that, at the threshold voltage of -5 V, the current jumps to a high value (the device is in a high-conducting state) and remains constant until an equal and reverse bias is applied ($+5$ V), whereupon it reverts to the initial value (the device is in a low-conducting state). This bistable behavior with a "pinch-off" in the I - V characteristics is a typical feature of a memristive device. From the plot of the ratio of the device currents in the ON and OFF states, it can be seen that the ratio is maximum at ± 3 V (operational voltage, SI Figure S7). For any practical application, the device can be switched ON by applying a bias voltage of more than -3 V.

The operational bias reduces to ± 2 V in the case of the 50 nm thick sandwich devices fabricated using the CP. If the switching behavior is field-induced, such a sandwich structure would show switching behavior in the millivolt regime, i.e. at a comparable field. Since field-induced modulation does not occur, the possibility of filamentary switching and conformational-change-induced switching is ruled out. The conductance jump is clearly a voltage-induced phenomenon. Hence, we state that the switching phenomenon is either redox-active or space-charge-induced; both of these behaviors are functions of the applied bias, and not the applied field. Scanning of the I - V curves for the sandwich and lateral devices at $V_{\text{max}} < \pm 2$ V and $V_{\text{max}} < \pm 3$ V, respectively, does not reveal any switching, and hence, the possibility of space-charge-induced switching, for which there is no threshold limit, is ruled out. This leaves only one possibility, redox-active switching.

The low-conducting-state current is termed as the OFF current or leakage current. From the plot of the ratio of the OFF current values for the CP and NCP devices against the applied bias, it can be seen that the leakage current of the CP device is 100 times lower than that of the NCP device. Therefore, we conclude that leakage current control in the CP is ~ 100 times more efficient than that in the NCP device (Figure 2b, SI Figure S8). In addition, when V_{\max} is increased, the CP device shows better control in restricting the leakage current over the NCP device. Note that leakage current control is one of the greatest challenges in the fabrication of state-of-the-art electronic devices. In principle, leakage current in the OFF state should be zero in a switching device. However, because of junction heating and stray noise, unwanted currents flow through the external circuit. If the polymer conductivity is low, heating at the junction contributes to an increase in the leakage current; on the other hand, if the conductivity is very high, stray noise passes through the material, thus increasing the leakage current. Therefore, it is critical to develop a material with moderate conductivity; this issue has been addressed by the synthetic route proposed in this study.

Our device can be switched ON at ± 3 V, where the leakage current is in the picoampere regime; this is $\sim 10^3$ times lower than that in the case of standard devices with comparable resistance. Hence, the amount of heat generated in our device is $\sim 10^6$ times lower ($H = i^2Rt$) than that in standard devices. The potential distribution in molecular structures can be determined by density functional simulation. In the present study, we find that the remarkable control of leakage current in the fabricated device is attributed to the fact that better conjugation (in the polymer) allows for efficient current flow through the conjugated chain in the matrix. Efficient transport of carriers enhances the growth/decay of induced charges around the Co atom of the CP matrix, and consequently, the amount of heat generated at the junction is very less. In contrast, in the case of the NCP matrix, the induced charges are localized and isolated, due to the capacitive effect being drastically weakened.⁴ The hysteresis area is directly proportional to the capacitive effect of a switching device. In addition, the isolation of “dielectric clusters” results in large-scale heat generation at the junction, and hence, the leakage current in an NCP device is increased.

The I – V characteristics of the free azo-ligand (SI Figure S5c) do not show any switching up to ± 16 V. Therefore, the results of CV and the direct switching response of the ligand-based device together suggest that the switching phenomenon shown by both polymers is due to the reduction of Co(III) to Co(II).

The ROM and RAM characteristics, which are typical to a memory device, are also investigated. The RAM (Figure 2c) and ROM (Figure 2d) of the CP device show reversible information processing and permanent memory storage capacities. To test the RAM, a write (-5 V)–read (-1 V)–erase ($+5$ V)–read (-1 V) cycle was sent through the device; only the read currents are plotted here. Note that it is possible to carry out RAM/ROM operations at $\pm 3, \pm 4, \pm 5, \pm 6, \pm 7, \pm 8, \pm 9, \pm 10, \pm 11, \pm 12, \pm 13, \pm 14$, and ± 15 V; therefore the CP device shows remarkable multilevel switching that can help replace the existing binary computing devices with a higher-logic system.²⁰ The ON/OFF ratio for the CP device is on the order of 10^2 , whereas that for NCP is < 10 . The ROM feature is several read currents (70 s) after writing a state once (solid circle), and then the same process is repeated after erasing once (hollow circle). The CP device was probed for more than 3 h, and it hardly showed any degradation

in its high (ON) and low (OFF) conducting state. The CP device shows unusually high robustness in air, and its retention time is considerably longer than that of the NCP device. The RAM and ROM behavior of the NCP device are given in SI Figure S9. Since no external signal is applied to the device when testing the ROM effect, the rapid weakening of the ROM effect in the NCP matrix clearly indicates that the spontaneous destruction of memory is due to the large leakage current generated by phonons and the subsequent isolation of clusters.

Generally it is believed that an increase in the matrix conductivity would lead to an increase in the OFF (leakage) and ON currents.^{7,11b} The fact is just opposite in molecular engineering. In other words, molecular engineering helps in blocking the leakage current and channeling it for stabilization of the ON and OFF states. Therefore, instead of metal ion doping to conducting polymers or inorganic semiconductors if a metal ion is bonded directly to the conjugated organic moiety, the leakage current tuning would enhance memristive features significantly.

■ ASSOCIATED CONTENT

S Supporting Information. Details of experimental procedure, NMR spectra, electrochemical data, AFM images. This material is available free of charge via the Internet at <http://pubs.acs.org>.

■ AUTHOR INFORMATION

Corresponding Author

HIGUCHI.Masayoshi@nims.go.jp

■ ACKNOWLEDGMENT

This work was financially supported by the Ministry of Education, Culture, Sports, Sciences, and Technology, Japan (MEXT), Japan Science and Technology Agency (JST) and New Energy and Industrial Technology Development Organization (NEDO). A part of this work was supported by the “Nanotechnology Network Project” of the Ministry of Education, Culture, Sports, Science and Technology (MEXT), Japan.

■ REFERENCES

- (1) Barabasi, A. L.; Butts, C. T.; Bascompte, J.; Ostrom, E.; Schweitzer, F.; Vespignani, A. *Science* **2009**, *325*, 405.
- (2) McGinnes, J.; Corry, P.; Proctor, P. *Science* **1974**, *183*, 853.
- (3) Chua, L. O. *IEEE Trans. Circuit Theory* **1971**, *18*, 507.
- (4) Strukov, D. B.; Snider, G. S.; Stewart, D. R.; Williams, R. S. *Nature* **2008**, *453*, 80.
- (5) (a) Ouyang, J.; Chu, C.; Szmanda, C. R.; Ma, L.; Yang, Y. *Nat. Mater.* **2004**, *3*, 918. (b) Chu, C. W.; Ouyang, J.; Tseng, J.-H.; Yang, Y. *Adv. Mater.* **2005**, *17*, 1440. (d) You, N.-M.; Chueh, C.-C.; Liu, C.-L.; Ueda, M.; Chen, W.-C. *Macromolecules* **2009**, *44*, 56.
- (6) (a) Ma, L.; Xu, Q.; Yang, Y. *Appl. Phys. Lett.* **2004**, *84*, 4908. (b) Lai, Y.-S.; Tu, C.-H.; Kwong, D.-L.; Chen, J. S. *Appl. Phys. Lett.* **2005**, *87*, 122101. (c) Joo, W. J.; Choi, T.-L.; Lee, J. H.; Lee, S. K.; Jung, M. S.; Kim, N.; Kim, J. M. *J. Phys. Chem. B* **2006**, *110*, 23812.
- (7) Bandyopadhyay, A.; Pal, A. *J. Appl. Phys. Lett.* **2004**, *84*, 999.
- (8) (a) Suppes, G. M.; Deore, B. A.; Freund, M. S. *Langmuir* **2008**, *24*, 1064. (b) Krieger, J. H.; Spitzer, S. *Switchable memory diode—a new memory device*. U.S. Patent 7,157,732, 2007. (c) Lai, Q.; Zhu, Z.; Chen, Y.; Patil, S.; Wudl, F. *Appl. Phys. Lett.* **2006**, *88*, 133513. (d) Krieger, J. H.; Trubin, S. V.; Vaschenko, S. B.; Yudanov, N. F. *Synth. Met.* **2001**, *122*, 199.
- (9) Barman, S.; Deng, F.; McCreery, R. L. *J. Am. Chem. Soc.* **2008**, *130*, 11073.

- (10) (a) Ma, L.; Pyo, S.; Ouyang, J.; Xu, Q.; Yang, Y. *Appl. Phys. Lett.* **2003**, *82*, 1419. (b) Kang, S. H.; Crisp, T.; Kymissis, I.; Bulovic, V. *Appl. Phys. Lett.* **2004**, *85*, 4666.
- (11) (a) Ling, Q.; Song, Y.; Ding, S. J.; Zhu, C.; Chan, D. S. H.; Kwong, D.-L.; Kang, E.-T.; Neoh, K.-G. *Adv. Mater.* **2005**, *17*, 455. (b) Bandyopadhyay, A.; Pal, A. J. *J. Phys. Chem. B* **2003**, *107*, 2531. (c) Kurokawa, H.; Lee, D.-S.; Watanabe, M.; Sagami, I.; Mikami, B.; Raman, C. S.; Shimizu, T. *J. Biol. Chem.* **2004**, *279*, 20186. (d) Green, J. E.; Wook Choi, J.; Boukai, A.; Bunimovich, Y.; Johnston-Halperin, E.; Delonno, E.; Luo, Y.; Sheriff, B. A.; Xu, K.; Shik Shin, Y.; Tseng, H.-R.; Stodart, J. F.; Heath, J. R. *Nature* **2007**, *445*, 414.
- (12) Martin, A. S.; Sambles, J. R.; Ashwell, G. J. *Phys. Rev. Lett.* **1993**, *70*, 218.
- (13) Ellenbogen, J. C.; Love, J. C. *Proc. IEEE* **2000**, *88*, 386.
- (14) Ling, Q.-D.; Liaw, D.-J.; Teo, E. Y.-H.; Zhu, C.; Chan, D. S.-H.; Kang, E.-T.; Neoh, K.-G. *Polymer* **2007**, *48*, 5182.
- (15) (a) Fang, J.; You, H.; Chen, J.; Lin, J.; Ma, D. *Inorg. Chem.* **2006**, *45*, 3701. (b) Choi, T.-L.; Lee, K.-H.; Joo, W.-J.; Lee, S.; Lee, T.-W.; Chae, M. Y. *J. Am. Chem. Soc.* **2007**, *129*, 9842. (c) Kim, K. K.; Joo, W.-J.; Song, E. S.; Kim, H. J.; Kim, J.; Park, C.; Lee, H. L.; Kim, C. *Synth. Met.* **2007**, *157*, 640. (d) Pradhan, B.; Das, S. *Chem. Mater.* **2008**, *20*, 1209.
- (16) (a) Ling, Q. D.; Kang, E.-T.; Neoh, K. G.; Chen, Y.; Zhuang, X. D.; Zhu, C. X. *Appl. Phys. Lett.* **2008**, *92*, 143302. (b) Ponomarev, Y. V.; Ivanov, S. A.; Rummyantsev, Y. A.; Gromchenko, A. A. *Quantum Electron* **2009**, *39*, 46.
- (17) Saha, A.; Ghosh, A. K.; Majumdar, P.; Mitra, K. N.; Mondal, S.; Rajak, K. K.; Falvello, L. R.; Goswami, S. *Organometallics* **1999**, *18*, 3772.
- (18) Saha, A.; Majumdar, P.; Goswami, S. *J. Chem. Soc., Dalton Trans.* **2000**, 1703.
- (19) Ling, Q.-D.; Liaw, D.-J.; Zhu, C.; Chan, D. S.-H.; Kang, E.-T.; Neoh, K.-G. *Prog. Polym. Sci.* **2008**, *33*, 917.
- (20) (a) Bandyopadhyay, A.; Miki, K.; Wakayama, Y. *Appl. Phys. Lett.* **2006**, *89*, 243506. (b) Bandyopadhyay, A.; Pati, R.; Sahu, S.; Peper, F.; Fujita, D. *Nat. Phys.* **2010**, *6*, 369.